Bioorganic & Medicinal Chemistry 20 (2012) 601–606

Contents lists available at ScienceDirect

Bioorganic & Medicinal Chemistry

journal homepage: www.elsevier.com/locate/bmc

A *para*-nitrophenol phosphonate probe labels distinct serine hydrolases of Arabidopsis

Sabrina Nickel [a], Farnusch Kaschani [b], Tom Colby [c], Renier A. L. van der Hoorn [b], Markus Kaiser [a,*]

[a] Zentrum für Medizinische Biotechnologie, Fakultät Biologie, Universität Duisburg-Essen, Universitätsstr. 2, D-45117 Essen, Germany
[b] The Plant Chemetics Laboratory, Chemical Genomics Centre of the Max Planck Society, Max Planck Institute for Plant Breeding Research, Carl-von-Linne-Weg 10, D-50829 Cologne, Germany
[c] Mass Spectrometry Group, Max Planck Institute for Plant Breeding Research, Carl-von-Linne-Weg 10, D-50829 Cologne, Germany

ARTICLE INFO

Article history:
Available online 15 July 2011

Keywords:
Activity-based protein profiling
Phosphonate probe
Paraoxon
Carboxylesterase
Nitrophenol
Arabidopsis thaliana

ABSTRACT

Activity-based protein profiling represents a powerful methodology to probe the activity state of enzymes under various physiological conditions. Here we present the development of a *para*-nitrophenol phosphonate activity-based probe with structural similarities to the potent agrochemical paraoxon. We demonstrate that this probes labels distinct serine hydrolases with the carboxylesterase CXE12 as the predominant target in *Arabidopsis thaliana*. The designed probe features a distinct labeling pattern and therefore represents a promising chemical tool to investigate physiological roles of selected serine hydrolases such as CXE12 in plant biology.

1. Introduction

Activity-based protein profiling (ABPP) is a powerful chemical biology methodology to probe the activity state and thus biological function of enzymes.[1] To this end, small molecules known as activity-based probes (ABPs) are applied to cell lysates, intact cells or even living organisms, where they react in an irreversible, covalent manner with their target enzymes. Labeled proteins are then detected and identified by a combination of protein gels and mass spectrometry. ABPs are composed of a 'warhead', that is, an irreversible, reactive enzyme inhibitor moiety, a tag such as biotin or the fluorophore rhodamine for purification and/or visualization, and a linker joining the two. While the ABPP methodology is well-established, a limitation of its scope is the number and labeling properties of currently available ABPs. To date, ABPs for several enzyme classes such as proteases, phosphatases or glycosidases have already been reported.[1,2] These ABPs however often differ in their in-class target selectivities: while some act as broadband probes, labeling a wide range of enzymes, others have rather narrow and thus highly-selective labeling properties. Broadband probes can be used to compare enzyme activity patterns of different biological samples; selective probes, in contrast, are powerful chemical tools for studying the function of a specific enzyme and are crucial for advanced applications such as activity-imaging.

In the last years, we have worked intensively to establish ABPP in plant biology research,[3] for example, by generating and establishing probes and protocols that have been used to elucidate the biological role of the pathogen-induced small molecule proteasome inhibitor Syringolin A.[4] However, further advancement of ABPP in plant biology is hampered by the limited availability of ABPs (both broadband and selective) with characterized labeling properties for plant proteomes.

Carboxylesterases (CXEs) are serine hydrolases present in all kingdoms of life with roles in diverse biological processes.[5] In plants, CXEs have been reported to participate in development, xenobiotic detoxification, secondary metabolism and defense.[6] CXEs have been labeled in ABPP studies with fluorophosphonate (FP)-based ABPs such as FP-Rh (**1**, Fig. 1),[7] but these are broadband probes labeling a multitude of other serine hydrolases in addition to several CXEs.[8] For ABPP-based functional studies of CXEs, more selective ABPs which only label predominantly distinct members within this serine hydrolase class therefore would be highly desirable. In 2007, the Baker group reported a co-complex structure of the *Actinidia eriantha* carboxylesterase CXE1 and the *p*-nitrophenyl phosphate agrochemical paraoxon (**2**, Fig. 1).[9] The structure revealed—as expected for a phosphate-based inhibitor—a covalent binding mode. It furthermore indicated that careful modifications of paraoxon could allow the generation of a CXE-targeting ABP. Here, we report the synthesis of a *para*-nitrophenol phosphonate-based ABP as a structural mimic of paraoxon and the subsequent identification of its corresponding targets in Arabidopsis leaf extracts.

* Corresponding author. Tel.: +49 201 183 2955; fax: +49 201 183 3672.
E-mail address: markus.kaiser@uni-due.de (M. Kaiser).

0968-0896/$ - see front matter © 2011 Elsevier Ltd. All rights reserved.
doi:10.1016/j.bmc.2011.06.041

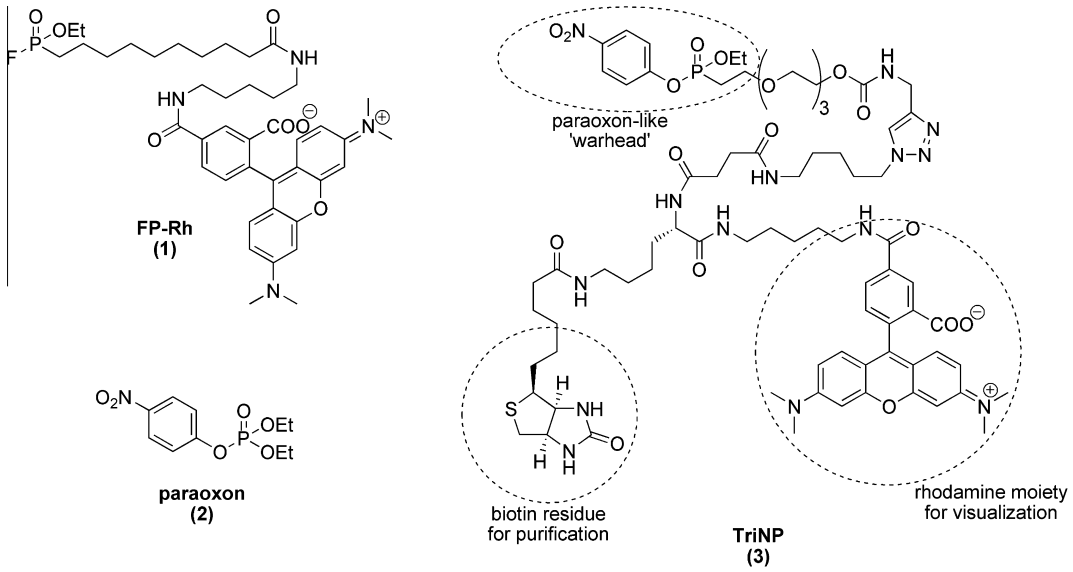

Figure 1. Chemical structures of the broadband serine hydrolase probe FP-Rh (**1**), of the agrochemical paraoxon (**2**), and of the designed trifunctional *para*-nitrophenol phosphonate TriNP (**3**).

2. Results and discussion

2.1. Design and chemical synthesis of a paraoxon-like *para*-nitrophenol phosphonate ABP

The X-ray structure of paraoxon (**2**, Fig. 1) bound to CXE1 revealed a diethyl phosphate moiety linked to the active site serine. Paraoxon's *para*-nitrophenol group, however, was absent, confirming its role as the leaving group during the covalent modification of the active site serine. Importantly, one of the ethoxy groups extends into the lipid binding cleft, indicating that replacement of this group with a suitably long linker, followed by a rhodamine visualization and biotin purification tag would not hamper binding efficiency. To limit unspecific binding and to ensure water solubility, a PEG linker was chosen. To incorporate the rhodamine and biotin tags, a Huisgen's [3+2] click chemistry approach was envisaged, making a modular synthesis of the desired ABP possible. These considerations led to the trifunctional *para*-nitrophenol phosphonate probe TriNP (Figs. 1 and 3). Although *para*-nitrophenol phosphonate-based probes have been reported,[10] a biotin- and rhodamine-containing ABP has (to the best of our knowledge) not yet been generated and tested on plant proteomes.

For the generation of the paraoxon-like phosphonate warhead, we followed in the first steps the previously reported FP-Rh synthesis strategy of Cravatt (Fig. 2).[8,11] To this end, commercially available tetraethylene glycol (**4**) was protected on one of its terminal hydroxyl groups as a *tert*-butyl dimethyl silyl ether, followed by conversion of the remaining hydroxyl group into an iodide residue. The resulting intermediate **6** was converted into the phosphonate **7** using standard Arbuzov conditions, followed by TBAF-mediated cleavage of the *tert*-butyl dimetyhl silyl protecting group. With the hydoxyl phosphonate **8** in hand, the reactive intermediate **9** was formed by reaction with *N*,*N*′-dihydroxysuccinimide carbonate. The subsequent addition of propargylamine led to urethane **10**, which upon treatment with oxalylchloride in diethyl ether resulted in chloro-phosphonate derivative **11**.[10] Treatment of this intermediate with *para*-nitrophenol and triethylamine in toluene finished the synthesis of the reactive *para*-nitrophenol phosphonate warhead of the ABP. Subsequent [3+2] Huisgen 'click' reaction of intermediate **12** with the trifunctional tag **13**[12] (which contains a fluorescent rhodamine moiety, a biotin residue for affinity purification and the azide functionality required for the click reaction) resulted in the generation of the desired target molecule TriNP (**3**).

2.2. Profiling and target identification with TriNP (3)

We first investigated the general target selectivity of our TriNP probe in Arabidopsis leaf extracts (Fig. 3A). To this end, Arabidopsis leaf extracts were preincubated with either 100 μM paraoxon or DMSO as a negative control for 30 min. Subsequently, a standard labeling experiment was performed with either the broadband serine hydrolase probe FP-Rh or with TriNP. As previously reported,[7] labeling with FP-Rh on leaf extracts resulted in a plethora of signals. Preincubation with paraoxon resulted in decreased FP-Rh signals predominantly in the 30 and 40 kDa region. Labeling with 2 μM TriNP, however, gave one major band at around 40 kDa, which was paraoxon-sensitive. These experiments revealed a significantly enhanced selectivity of TriNP when compared to FP-Rh. Importantly, all TriNP-derived signals were competable by preincubation with paraoxon, demonstrating that the attachment of the linker and of the biotin/rhodamine-tags did not lead to unspecific labelling.

We next identified TriNP-labeled proteins in Arabidopsis leaf extracts using affinity purification on avidin beads. After labeling of the extracts with 5 μM of TriNP, affinity capture, and separation on SDS protein gels, fluorescent bands were excised from the gel and *in gel*-digested with trypsin.

NanoLC-ESI-MS/MS-analysis identified CXE12 as the predominant target. Several other serine hydrolases [tripeptidyl-peptidase 2 (TPP2), prolyloligopeptidase-like (POPL), serine carboxylpeptidase 48 (SCPL48) and carboxylesterase 7 (CXE7)] were identified as well, consistent with a phosphonate-based ABP (Fig. 3B, Supplementary Fig. 1 and Table 1).[7,8] Interestingly, no signals could be visualized in the 30 kDa region, even though preincubation with paraoxon indicated a 30 kDa putative paraoxon target (Fig. 3). The most likely target of FP in this region is the methylesterase MES2.[7,13] Crystallographic studies on a MES2 homolog from *Nicotiana tabacum* however indicate that the active site pocket of this enzyme has strict size limitations.[6a] In order to investigate if the observed target selectivity from TriNP results from the bulky rhodamine and biotin tags, we performed an additional 2-step labeling strategy, using alkyne **12** as an ABP and click chemistry

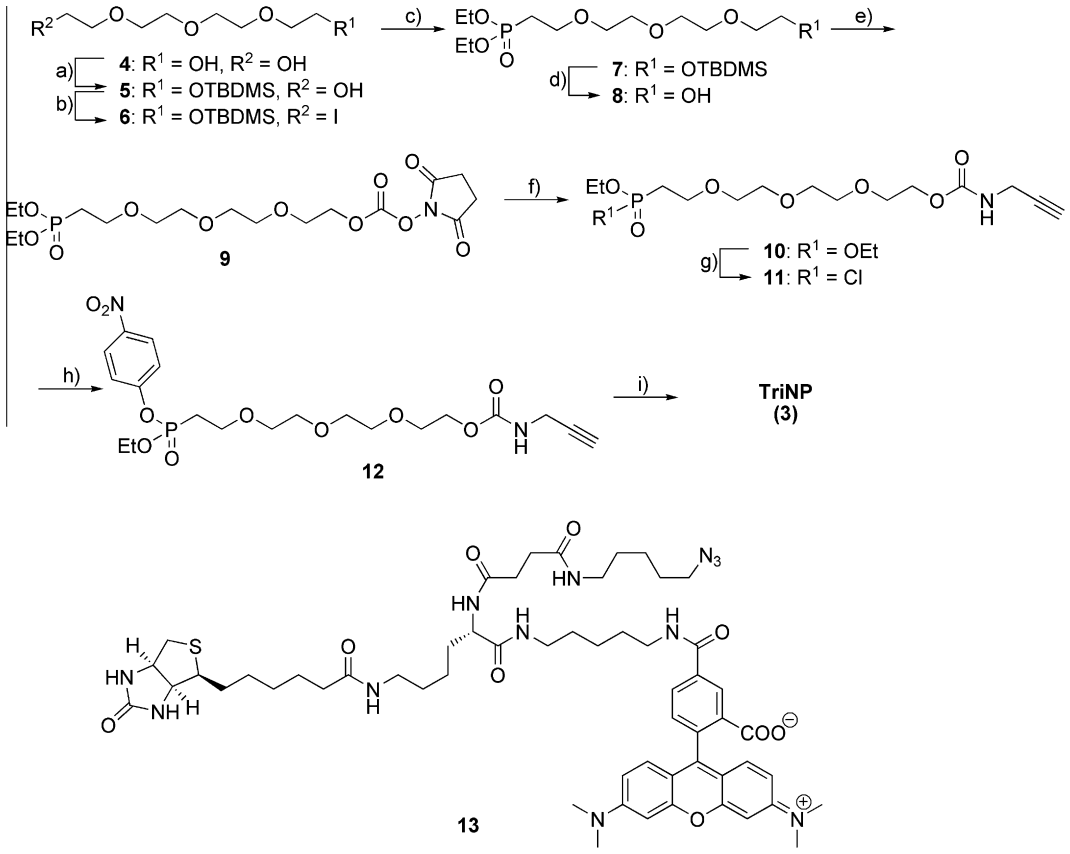

Figure 2. Chemical synthesis of the ABP TriNP (**3**). (a) TBDMS–Cl, imidazole, DCM, rt, 12 h, 43%; (b) I_2, PPh_3, imidazole, toluene, rt, 1.5 h, 77%; (c) $P(OEt)_3$, 150 °C, 1 h, 91%; (d) TBAF, THF, 0 °C to rt, 12 h, 73%; (e) *N,N′*-disuccinimidyl carbonate, NEt_3, DMF, rt, 12 h, 49%; (f) propargylamine, $NaHCO_3$, MeOH, rt, 12 h, 80%; (g) oxalyl chloride, DCM, rt, 12 h, 99%; (h) *para*-nitrophenol, NEt_3, toluene, rt, 3 h, 40%; (i) **13**, TCEP, TBTA, $CuSO_4$, H_2O, rt, 12 h, 28%.

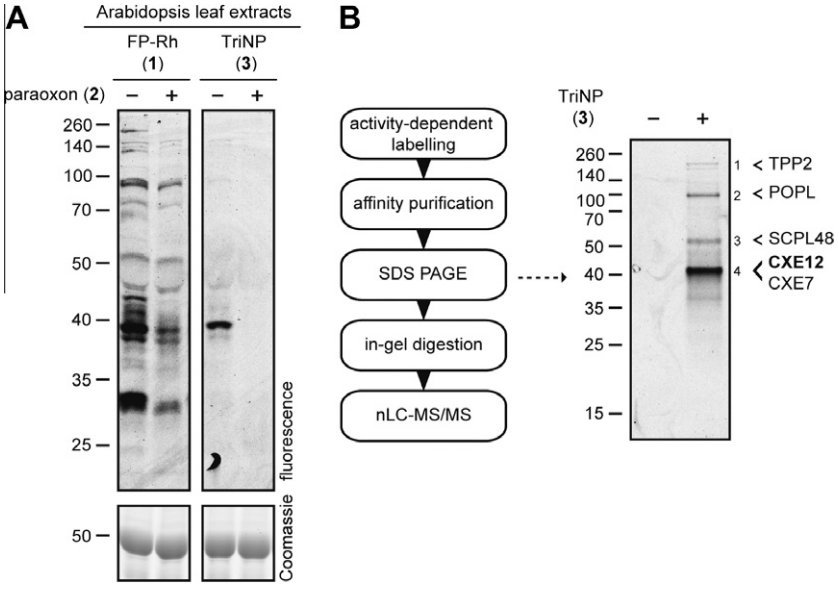

Figure 3. TriNP is more specific than FP-Rh and predominantly labels the serine hydrolase CXE12. (A) An extract from *Arabidopsis thaliana* leaves was preincubated with 100 μM paraoxon or DMSO for 30 min, followed by the addition of either 2 μM FP-Rh or 2 μM TriNP for 1 h. The reaction was stopped by addition of 4× gel loading buffer. Proteins were separated on protein gels, and fluorescent signals were detected by fluorescence scanning. (B) Affinity purification of TriNP targets and subsequent identification by nanoLC-ESI-MS/MS. Labeled proteins were affinity purified on avidin beads after activity-dependent labeling with 5 μM TriNP. The purified proteins were then separated by SDS–PAGE and visualized with a fluorescent scanner. Fluorescent gel regions were excised and subjected to in-gel digestion with trypsin. The obtained peptides were analyzed by nanoLC-ESI-MS/MS.

with **13** after labeling to visualize labeled proteins (Supplementary Fig. 2). The 2-step labeling profile is highly similar to the one from TriNP. Only TPP2 was less efficiently labelled, most probably as a result of the overall lower labeling efficiency resulting from the additional click chemistry step. We therefore propose that the observed enhanced target selectivity of TriNP versus FP-Rh is a conse-

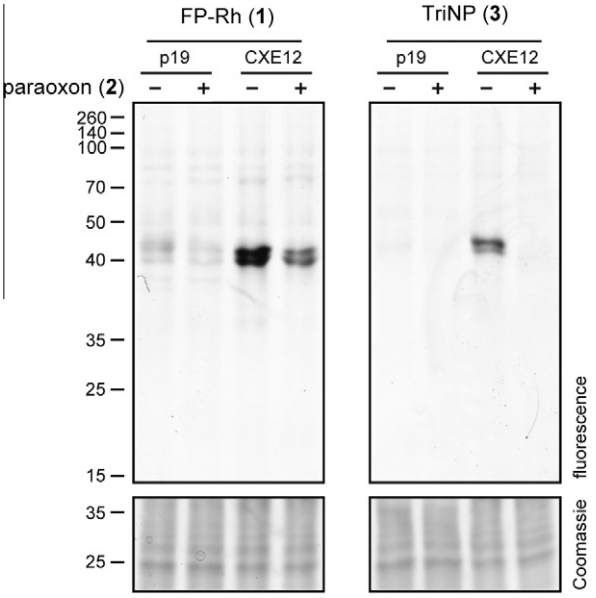

Figure 4. Specific labeling of agroinfiltrated CXE12. Extracts from agroinfiltrated leaves overexpressing CXE12 with silencing suppressor p19 or p19 alone were preincubated for 30 min with or without 100 μM paraoxon and labeled with 2 μM FP-Rh or TriNP for 1 h. After separation on a protein gel, fluorescent labeled proteins were visualized with a fluorescence scanner.

quence of either the change of the leaving group on the phosphonate moiety and/or the substitution of the alkyl to a PEG linker.

To confirm the labeling of CXE12 by the paraoxon-derived probe, we performed labeling experiments with CXE12 transiently overexpressed in *Nicotiana benthamiana*. The CXE12 cDNA was cloned into a binary vector which was used to transform *Agrobacterium tumefaciens*. Cultures of the *A. tumefaciens* strain carrying CXE12 were then mixed with strains carrying the RNA silencing inhibitor p19 and co-infiltrated into *N. benthamiana* leaves.[7,14] As a negative control for this experiment, we also infiltrated leaves with only the silencing suppressor p19. At 5 days post-infiltration, leaves were harvested and used for labeling studies. Preincubation of leaf extracts from CXE12 overexpressing leaves as well as preincubation of extracts of leaves expressing only the p19 suppressor with either paraoxon or DMSO, confirmed that CXE12 is a target of TriNP (Fig. 4). The molecular basis of the double CXE12 signal is unknown at this stage.

3. Conclusions

Our studies have resulted in the development of a paraoxon-like *para*-nitrophenol phosphonate ABP that labels predominantly CXE12 in *Arabidopsis*. CXE12 has specifically been implicated in bioactivation of herbicides, for example, by hydrolysis of the pro-herbicide methyl-2,4-dichlorphenoxyacetate into the phytotoxic agent 2,4-dichlorophenoxy acetic acid.[6c] Besides its role in bioherbicide activation, no other biological roles of CXE12 are known. The ABP TriNP (**3**) could therefore represent a promising chemical tool to further investigate the function of CXE12 due to its altered, highly specific labeling profile. In this context it should be noted that a probe for labeling CXE12 has recently been reported which, however, requires cautious use due to potential problems with labeling intensity and off-target labelling.[15]

Interestingly, a previous study on *para*-nitrophenol phosphonate-based inhibitors demonstrated that this type of warhead also inhibits cutinases.[10] Plant pathogens often employ cutinases during infection.[16] Consequently, TriNP (**3**) might also find important applications in plant-pathogen studies.

4. Experimental

4.1. General

All reagents were purchased with highest purity available from Sigma–Aldrich, Acros, Fisher Scientific, Merck, or Fluka, and were used without further purification. Anhydrous, as well as p.a. grade solvents, were purchased from commercial suppliers. All reactions were carried out under an argon atmosphere. Flash silica gel chromatography was performed with silica gel from Acros (particle size 35–70 μm) and Li-Chroprep RP 18 from Merck (particle size 40–63 μm). Thin layer chromatography (TLC) was carried out on Merck aluminium precoated silica gel plates (20 × 20 cm, $60F_{254}$ and 60 RP-18 $F_{254}S$) using UV irradiation at 254 and 366 nm or the following developing reagents (Reagent A: 20 g of phosphomolybdic acid hydrate in 80 mL ethanol, Reagent B: 1.5 g $KMnO_4$, 10 g K_2CO_3 and 1.25 mL of 10% aq NaOH in 200 mL water). Eluents and R_f values are given in the respective experiment. LC–MS analyses were performed on a HPLC system from Agilent (1200 series) with an Eclipse XDB-C18, 5 μm column from Agilent (peak detection at 210 nm) and a Thermo Finnigan LCQ Advantage Max ESI-Spectrometer. A linear gradient of solvent B (0.1% formic acid in acetonitrile) in solvent A (0.1% formic acid in water) was used at 1 mL/min flow rate. Nuclear magnetic resonance (NMR) spectra were recorded on a Varian Mercury 400 system (400 MHz for ^{1}H-, 100 MHz for ^{13}C-, and 162 MHz for ^{31}P-NMR), a Bruker Avance DRX 500 system (500 MHz for ^{1}H- and 126 MHz for ^{13}C-NMR) or a Varian Unity Inova 600 system (600 MHz for ^{1}H- and 151 MHz for ^{13}C-NMR). ^{1}H NMR spectra are reported in the following manner: chemical shifts (δ) in ppm calculated with reference to the residual signals of undeuterated solvent, multiplicity (s, singlet; d, doublet; t, triplet; dt, doublet of triplet; m, multiplet), coupling constants (J) in Hertz (Hz), and number of protons (H).

4.2. Synthesis

4.2.1. Synthesis of 2,2,3,3-tetramethyl-4,7,10-13-tetraoxa-3-silapentadecan-15-ol (5)

To a solution of tetraethylene glycol (**4**) (10 g, 51.5 mmol) in DCM (80 mL) was added imidazole (7 g, 103 mmol, 2 equiv) and TBDMS–Cl (7.8 g, 51.5 mmol, 1 equiv), and the resulting solution was stirred over night at room temperature. The reaction was quenched by addition of saturated aq $NaHCO_3$, and extracted twice with ethyl acetate. The combined organic phases were washed with brine and the organic phase was dried over sodium sulfate. After purification on silica gel column (cyclohexane/ethyl acetate 1:2), 6.7 g (22.1 mmol, 43%) of the desired product **5** was isolated. ^{1}H NMR ($CDCl_3$) δ 3.75 (t, 2H, J = 5.4 Hz), 3.71 (m, 2H), 3.65 (d, 8H, J = 4.3 Hz), 3.59 (m, 2H), 3.54 (t, 2H, J = 5.4 Hz), 0.88 (s, 9H), 0.05 (s, 6H); ^{13}C NMR ($CDCl_3$) δ 72.6, 70.8, 70.5, 62.8, 61.9, 26.1, 18.5, −5.2; TLC (cylohexane/ethyl acetate 1:2) R_f = 0.25; ESI-MS: t_R 4.21 min, m/z 308.87 $[M+H]^+$, 309.21 calcd for $C_{14}H_{33}O_5Si^+$.

4.2.2. Synthesis of 15-Iodo-2,2,3,3-tetramethyl-4,7,10,13-tetraoxa-3-silapentadecane (6)

To a solution of **5** (6.0 g, 19.7 mmol) in toluene (150 mL) was added triphenylphosphine (25.8 g, 98.5 mmol, 5 equiv), iodine (20.0 g, 78.8 mmol, 4.5 equiv) and imidazole (7.0 g, 102.4 mmol, 5.2 equiv). The heterogenic solution was stirred for 1.5 h at room temperature and was then filtered and washed with ethyl acetate. A saturated aq sodium thiosulfate solution was added, the organic phase was washed with water and brine, and the organic phase was dried over sodium sulfate. After silica gel chromatography (cyclohexane/ethyl acetate 5:1), 6.3 g (15.1 mmol, 77%) of the desired product **6** was isolated. ^{1}H NMR ($CDCl_3$): δ 3.78–3.73

(m, 4H), 3.65 (m, 8H), 3.55 (t, 2H, J = 5.4 Hz), 3.25 (t, 2H, J = 7.0 Hz), 0.88 (s, 9H), 0.05 (s, 6H); ^{13}C NMR ($CDCl_3$): δ 72.8, 72.1, 70.9, 70.8, 70.4, 26.1, 18.5, 3.1, −5.1; TLC (cyclohexane/ethyl acetate 5:1): R_f = 0.35; ESI-MS: t_R 4.31 min, m/z 419.20 $[M+H]^+$, 419.11 calcd for $C_{14}H_{33}IO_4Si^+$.

4.2.3. Synthesis of diethyl(2,2,3,3-tetramethyl-4,7,10,13-tetraoxa-3-silapentadecan-15-yl-phosphonate (7)

Compound **6** (5.5 g, 13.1 mmol) was dissolved in $P(OEt)_3$ (12.4 mL, 71 mmol, 5.4 equiv) and heated up to 150 °C and stirred for 1 h at this temperature. The excess of $P(OEt)_3$ was subsequently removed in high vacuum and the residue purified on silica gel column (DCM/methanol 50:1), yielding 5.1 g (12 mmol, 91%) of the desired product **7**. ^{1}H NMR ($CDCl_3$): δ 4.14–4.03 (m, 4H), 3.73 (m, 4H), 3.65–3.58 (m, 8H), 3.54 (t, 2H, J = 5.4 Hz), 2.16–2.07 (m, 2H), 1.30 (t, 6H, J = 7.1 Hz), 0.88 (s, 9H), 0.05 (s, 6H); ^{13}C NMR ($CDCl_3$): δ 72.8, 70.9, 70.6, 70.3, 65.3, 62.8, 61.8, 27.8, 26.4, 26.1, 16.6, −5.1; ^{31}P NMR ($CDCl_3$): δ 29.6; TLC (DCM/methanol 50:1): R_f = 0.20; ESI-MS: t_R 4.32 min, m/z 429.20 $[M+H]^+$, 429.25 calcd for $C_{18}H_{42}O_7PSi^+$.

4.2.4. Synthesis of diethyl(2-(2-(2-(2-hydroxyethoxy)ethoxy) ethoxy)ethyl)phosphonate (8)

A solution of **7** (5.1 g, 12.0 mmol) in THF (150 mL) was cooled to 0 °C and TBAF (13.1 mL of a 1 M solution in THF, 14.0 mmol, 1.25 equiv) was added slowly. The resulting mixture was stirred over night and warmed to room temperature. The reaction was quenched by addition of water and the resulting mixture was extracted three times with DCM. Drying of the organic phase over sodium sulfate and purification by silica gel chromatography (DCM/methanol 19:1) led to 2.8 g (8.8 mmol, 73%) of the desired product **7**. ^{1}H NMR ($CDCl_3$): δ 4.13–4.03 (m, 4H), 3.75–3.57 (m, 14 H), 2.12 (dt, 2H, J = 18.8, 7.6 Hz), 1.30 (t, 6H, J = 7.1 Hz); ^{13}C NMR ($CDCl_3$): δ 72.7, 70.7, 70.5, 70.2, 65.3, 61.8, 27.7, 26.4, 16.6; TLC (DCM/MeOH 19:1): R_f = 0.40; ESI-MS: t_R 4.31 min, m/z 315.13 $[M+H]^+$, 315.16 calcd for $C_{12}H_{28}O_7P^+$.

4.2.5. Synthesis of 2-(2-(2-(2-(diethoxyphosphoryl)ethoxy) ethoxy)ethoxy)ethyl(2,5-dioxopyrrolidin-1-yl)carbonate (9)

Compound **8** (2.0 g, 6.4 mmol) was dissolved in DMF (18.7 mL, 0.34 M) and *N*,*N*′-disuccinimidyl carbonate (3.6 g, 14.1 mmol, 2.2 equiv) and NEt_3 (2.2 mL, 16.0 mmol, 2.5 equiv) were added. The resulting mixture was stirred over night at room temperature. Water and DCM were added and the organic and water phase were separated. The organic layer was washed three times with brine, separated and the organic phase was dried over sodium sulfate. After silica gel chromatography (DCM/methanol 50:1), 1.44 g (3.2 mmol, 49%) of the desired product **9** was obtained. ^{1}H NMR ($CDCl_3$): δ 4.45–4.42 (m, 2H), 4.12–4.03 (m, 4H), 3.79–3.57 (m, 12H), 2.82 (s, 4H), 2.11 (dt, 2H, J = 18.7, 7.6 Hz), 1.29 (t, 6H, J = 7.1 Hz); ^{13}C NMR ($CDCl_3$): δ 168.7, 151.7, 71.0, 70.7, 70.3, 68.4, 65.2, 61.8, 27.7, 25.6, 16.6; TLC (DCM/methanol 50:1): R_f = 0.20; ESI-MS: t_R 4.21 min, m/z 456.20 $[M+H]^+$, 455.16 calcd for $C_{17}H_{31}NO_{11}P^+$.

4.2.6. Synthesis of 2-(2-(2-(2-(diethoxyphophoryl)ethoxy) ethoxy) ethoxy)ethyl prop-2-yn-1-yl carbamate (10)

To a solution of **9** (405.5 mg, 0.89 mmol) in methanol (5 mL) were added propargylamine (73.5 mg, 1.3 mmol, 1.5 equiv) and sodium bicarbonate and the resulting mixture was stirred over night at room temperature. The solvent was evaporated and purification on silica gel column ($CHCl_3$/methanol 19:1) yielded 281.1 mg (0.71 mmol, 80%) of the desired product **10**. ^{1}H NMR ($CDCl_3$): δ 4.26–4.21 (m, 2H), 4.14–4.04 (m, 4H), 3.95 (s, 2H), 3.76–3.59 (m, 12H), 2.22 (t, 1H, J = 2.3 Hz), 2.12 (dt, 2H, J = 18.7, 7.5 Hz), 1.31 (t, 6H, J = 7.1 Hz); ^{13}C NMR ($CDCl_3$): δ 162.7, 79.9, 71.5, 70.7, 70.3, 69.6, 65.2, 64.4, 61.9, 30.9, 27.8, 16.6; TLC ($CHCl_3$/methanol 19:1): R_f = 0.30; LC–MS (ESI): t_R 7.19 min, m/z 396.00 $[M+H]^+$, 396.18 calcd for $C_{16}H_{31}NO_8P^+$.

4.2.7. Synthesis of 2-(2-(2-(2-(chloro)ethoxy)phosphory)ethoxy) ethoxy)ethoxy)ethyl prop-2-yn-1-yl carbamate (11)

To a solution of **10** (80 mg, 0.2 mmol) in DCM (1 mL) was added dropwise oxalyl chloride (0.34 ml, 4.0 mmol, 20 equiv) and the resulting mixture was stirred over night at room temperature. The solvent was removed under a stream of argon and dried under high vacuum. The remaining residue **11** (76.4 mg, 0.19 mmol, 99%) was used in the next step without any further purification. ^{1}H NMR ($CDCl_3$): δ4.51–4.45 (m, 3H), 4.42–4.18 (m, 3H), 3.89–3.75 (m, 4H), 3.69–3.61 (m, 8H), 2.53 (dt, 2H, J = 18.1, 7.4 Hz), 2.32 (t, 1H, J = 2.4 Hz), 1.39 (t, 3H, J = 7.1 Hz); ^{13}C NMR ($CDCl_3$): δ 152.1, 76.4, 73.0, 70.8, 70.7, 70.6, 68.4, 68.1, 64.6, 35.4, 33.2, 16.1; ^{31}P NMR ($CDCl_3$): δ 40.6.

4.2.8. Synthesis of 2-(2-(2-(2-(ethoxy(4-nitrophenoxy) phosphoryl)ethoxy)ethoxy)ethoxy)ethyl prop-2-yn-1-yl carbamate (12)

To a solution of **11** (76.4 mg, 0.19 mmol) in toluene (1 mL) was added dropwise a solution of *para*-nitrophenol (55.6 mg, 0.38 mmol, 2 equiv) and triethylamine (0.14 mL, 0.95 mmol, 5 equiv) in toluene (1 mL). The resulting mixture was stirred for 3 h at room temperature and then evaporated to dryness. The subsequent purification by silica gel column chromatography ($CHCl_3$/methanol 50:1) yielded 38.7 mg (0.08 mmol, 40%) of the desired product **12**. ^{1}H NMR ($CDCl_3$): δ 8.23 (d, 2H, J = 9.2 Hz), 7.39 (d, 2H, J = 9.2 Hz), 4.30–4.14 (m, 4H), 3.96 (d, 2H, J = 2.5 Hz), 3.87–3.77 (m, 2H), 3.69–3.65 (m, 2H), 3.61 (d, 8H, J = 6.5 Hz), 2.33 (dt, 2H, J = 18.6, 7.1 Hz), 2.22 (t, 1H, J = 2.4 Hz), 1.32 (t, 3H, J = 7.1 Hz); ^{13}C NMR ($CDCl_3$): δ 155.7, 155.3, 144.7, 125.8, 121.3, 78.9, 71.6, 70.7, 70.5, 69.6, 64.8, 64.4, 63.4, 30.9, 28.2, 16.5; ^{31}P NMR ($CDCl_3$): δ 28.0; TLC ($CHCl_3$/methanol 50:1): R_f = 0.06; LC–MS (ESI): t_R 8.58 min, m/z 489.00 $[M+H]^+$, 489.17 calcd for $C_{20}H_{30}N_2O_{10}P^+$.

4.2.9. Synthesis of TriNP (3)

To a solution of **12** (0.4 mg, 0.9 μmol) and **13** (1 mg, 0.9 μmol) in water (0.3 mL) was added TCEP (3 μL of a 50 mM solution in water, 0.15 μmol, 0.25 equiv), TBTA (3 μL of a 100 mM solution in DMSO, 0.3 μmol, 0.5 equiv) and $CuSO_4$ (30 μL of a 5 mM solution in water, 0.15 μmol, 0.25 equiv). The resulting mixture was stirred in the dark over night at room temperature. The mixture was evaporated to dryness and the crude residue was purified by C18 reversed phase silica gel (water with 20% CH_3CN–50% CH_3CN) to yield 0.4 mg (0.26 mmol, 28%) of the desired product **3**. TLC (CH_3CN/water 1:1): R_f = 0.45; LC–MS (ESI): t_R 7.48 min, m/z 1567.60 $[M+H]^+$, 1589.53 $[M+Na]^+$, 784.80 $[M+2H]^{2+}$, 1567.71 calcd for $C_{75}H_{104}N_{14}O_{19}PS^+$.

4.3. Profiling and target identification

4.3.1. Sample preparation

Arabidopsis thaliana leaf extracts were obtained by grinding 2 g of frozen leaves of 4-week-old *A. thaliana* ecotype Col-0 in a mortar at room temperature (22–24 °C) to a homogenous green paste. The paste was mixed with 5–6 mL of distilled water and cleared by centrifugation (5 min at 16,000×g). The protein concentration was determined by using the Reducing agent Compatible/Detergent Compatible (RC/DC) Protein Assay (Bio-Rad) following the manufacturer's instructions.

Full-length CXE12 (At3g48690) cDNA was amplified from an *A. thaliana* cDNA library (kindly provided by Dr. Hans Sommer, Max Planck Institute for Plant Breeding Research) using the primers

r434 (forward, 5′-GAT CCC ATG GAT TCC GAG ATC GCC GTC GAC-3′) and r435 (reverse, 5′-GAT CCT GCA GCT AGT TCC CTC CCT TAA TAA ACC C-3′). The fragment was cloned into the cloning vector pFK26 using the NcoI and PstI restriction sites, resulting in pFK161.[17] The 35S::CXE12::terminator cassette was excised from pFK161 with XbaI and EcoRI and shuttled into pTP5.[17] The resulting binary vector pBP8 was transformed into *A. tumefaciens* strain GV3101 pMP90.[18] Transient overexpression of CXE12 was achieved by co-infiltrating cultures of *Agrobacterium* strains carrying pBP8 together with cultures carrying silencing inhibitor p19 in fully expanded leaves of 4-week-old *N. benthamiana*.[14] Leaves were harvested after 3 days, and the proteins were extracted as described above.

4.3.2. Sample preparation for target identification

The labeling reactions and the affinity purification of labeled target proteins was carried out as previously described.[7] Affinity purified, labeled target proteins were separated by 1D SDS–PAGE and visualized on a Typhoon 8600 (GE Healthcare, Pittsburgh, USA) fluorescence scanner. Fluorescent areas were cut out with a disposable steel blade and washed several times with water. The gel slices were then subjected to the in-gel-digestion procedure and obtained peptides used for the subsequent nanoLC-ESI-MS/MS analysis.[7]

4.4. Mass spectrometry

Experiments were performed on a Thermo LTQ Velos mass spectrometer coupled to a Proxeon EASY-nLC. The LTQ Velos mass spectrometer was operated using Xcalibur software (version 2.1). The mass spectrometer was set in the positive ion mode, survey scanning between *m/z* of 400 and 1600, with an ionization potential of 3.61 kV. Peptides were separated on a single reverse phase C_{18} column (inner diameter 75 μm, packed with 12 cm ReproSil-Pur C_{18}-AQ (3 μm)) using an acetonitrile gradient (5–40% over 90 min), at a flowrate of 300 nL/min. Peptides were fragmented by collision-induced decay (CID) in a data-directed fashion, fragmenting the 20 most intense multiply-charged precursors in each MS scan. CID collision energy was set to 35% for the generation of MS2 spectra. Following fragmentation, precursors were excluded from further MS/MS acquisition for 60 s with a list of excluded ions consisting of 500 members maximum.

4.4.1. Peptide and protein Identification

MS2 spectra data were searched using the SEQUEST algorithm as implemented in the Thermo Proteome Discoverer software (version 1.2) against a custom-made database containing *A. thaliana* sequences from the TAIR10_pep_20101028.fasta database (version October 2010, www.arabidopsis.org). In order to increase the statistical significance of peptide matches, the database was supplemented with *Pseudomonas aeruginosa* sequences from the Pseudomonas_aeruginosa_PAO1.txt (version November 2009, www.pseudomonas.com) and sequences for chicken avidin, human keratins and porcine trypsin (the latter sequences were obtained from SwissProt). In total the search database contained 41012 protein sequence entries. SEQUEST searches allowed for oxidation of methionine residues (16 Da), static modification of cysteine residues (57 Da; due to alkylation), tryptic peptides with one missed cleavage allowed, and a mass tolerance set to ±0.25 Da for precursor mass and ±0.8 Da for product ion masses. The ‘Decoy Database Search’ was turned on.

The resulting MS2 spectra matches were assembled and filtered in Proteome Discoverer. Spectra matches were retained when their confidence score was ‘medium’ or ‘high’. Protein identification required the matching of at least two peptides per protein not shared with any other unrelated protein in the database (matches to isoforms coming from the same gene locus were allowed).

Acknowledgements

The authors would like to thank Bikram Pandey for providing pBP8 and Sarah Tully and Benjamin F. Cravatt for a kind donation of FP-Rh. Support of this work by the Deutsche Forschungsgemeinschaft (KA 2894/1-1 to M.K., HO 3983/3-2 and HO3983/4-1 to R.H.) is greatly acknowledged.

Supplementary data

Supplementary data associated with this article can be found, in the online version, at doi:10.1016/j.bmc.2011.06.041.

References and notes

1. (a) Cravatt, B. F.; Wright, A. T.; Kozarich, J. W. *Annu. Rev. Biochem.* **2008**, *77*, 383; (b) Sadaghiani, A. M.; Verhelst, S. H. L.; Bogyo, M. *Curr. Opin. Chem. Biol.* **2007**, *11*, 20.
2. Barglow, K. T.; Cravatt, B. F. *Nat. Methods* **2007**, *4*, 822.
3. (a) Wang, Z.; Gu, C.; Colby, T.; Shindo, T.; Balamurugan, R.; Waldmann, H.; Kaiser, M.; van der Hoorn, R. A. L. *Nat. Chem. Biol.* **2008**, *4*, 557; (b) Kaschani, F.; Verhelst, S. H. L.; van Swieten, P. F.; Verdoes, M.; Wong, C.-S.; Wang, Z.; Kaiser, M.; Overkleeft, H. S.; Bogyo, M.; van der Hoorn, R. A. L. *Plant J.* **2009**, *57*, 373; (c) Kolodziejek, I.; van der Hoorn, R. A. L. *Curr. Opin. Biotechnol.* **2010**, *21*, 225.
4. (a) Kolodziejek, I.; Misas-Villamil, J. C.; Kaschani, F.; Clerc, C.; Gu, C.; Krahn, D.; Niessen, S.; Verdoes, M.; Willems, L. I.; Overkleeft, H. S.; Kaiser, M.; van der Hoorn, R. A. L. *Plant Physiol.* **2011**, *155*, 477; (b) Groll, M.; Schellenberg, B.; Bachmann, A. S.; Archer, C. R.; Huber, R.; Powell, T. K.; Lindow, S.; Kaiser, M.; Dudler, R. *Nature* **2008**, *452*, 755; (c) Clerc, J.; Groll, M.; Nukic, D.; Bachmann, A. S.; Huber, R.; Schellenberg, B.; Dudler, R.; Kaiser, M. *Proc. Natl. Acad. Sci. U.S.A.* **2009**, *106*, 6507; (d) Clerc, J.; Florea, B. I.; Kraus, M.; Groll, M.; Huber, R.; Bachmann, A. S.; Dudler, R.; Driessen, C.; Overkleeft, H. S.; Kaiser, M. *Chembiochem* **2009**, *10*, 2638.
5. Satoh, T.; Hosokawa, M. *Annu. Rev. Pharmacol. Toxicol.* **1998**, *38*, 257.
6. (a) Forouhar, F.; Yang, Y.; Kumar, D.; Chen, Y.; Fridman, E.; Park, S. W.; Chiang, Y.; Acton, T. B.; Montelione, G. T.; Pichersky, E.; Klessig, D. F.; Tong, L. *Proc. Natl. Acad. Sci. U.S.A.* **2005**, *102*, 1773; (b) Ueguchi-Tanaka, M.; Ashikari, M.; Nakajima, M.; Itoh, H.; Katoh, E.; Kobayashi, M.; Chow, T.; Hsing, Y. C.; Kitano, H.; Yamaguchi, I.; Matsuoka, M. *Nature* **2005**, *437*, 693; (c) Gershater, M. C.; Cummins, I.; Edwards, R. *J. Biol. Chem.* **2007**, *282*, 21460; (d) Marshall, S. D. G.; Putterill, J. J.; Plummer, K. M.; Newcomb, R. D. *J. Mol. Evol.* **2003**, *57*, 487; (e) Gershater, M. C.; Edwards, R. *Plant Sci.* **2007**, *173*, 579.
7. Kaschani, F.; Gu, C.; Niessen, S.; Hoover, H.; Cravatt, B. F.; van der Hoorn, R. A. L. *Mol. Cell. Proteomics* **2009**, *8*, 1082.
8. (a) Liu, Y.; Patricelli, M. P.; Cravatt, B. F. *Proc. Natl. Acad. Sci. U.S.A.* **1999**, *96*, 14694; (b) Simon, G. M.; Cravatt, B. F. *J. Biol. Chem.* **2010**, *285*, 11051.
9. Ileperuma, N. R.; Marshall, S. D. G.; Squire, C. J.; Baker, H. M.; Oakeshott, J. G.; Russell, R. J.; Plummer, K. M.; Newcomb, R. D.; Baker, E. N. *Biochemistry* **2007**, *46*, 1851.
10. (a) Dijkstra, H. P.; Sprong, H.; Aerts, B. N. H.; Kruithof, C. A.; Egmond, M. R.; Klein Gebbink, R. J. M. *Org. Biomol. Chem.* **2008**, *6*, 523; (b) Wieczorek, B.; Lemcke, B.; Dijkstra, H. P.; Egmond, M. R.; Klein Gebbink, R. J. M.; van Koten, G. *Eur. J. Inorg. Chem.* **2010**, 1929.
11. Kidd, D.; Liu, Y.; Cravatt, B. F. *Biochemistry* **2001**, *40*, 4005.
12. Speers, A. E.; Adam, G. C.; Cravatt, B. F. *J. Am. Chem. Soc.* **2003**, *125*, 4686.
13. Vlot, A. C.; Liu, P. P.; Cameron, R. K.; Park, S. W.; Yang, Y.; Kumar, D.; Zhou, F.; Padukkavidana, T.; Gustafsson, C.; Pichersky, E.; Klessig, D. F. *Plant J.* **2008**, *56*, 445.
14. Voinnet, O.; Rivas, S.; Mestre, P.; Baulcombe, D. *Plant J.* **2003**, *33*, 949.
15. Sellars, J. D.; Landrum, M.; Congreve, A.; Dixon, D. P.; Mosely, J. A.; Beeby, A.; Edwards, R.; Steel, P. G. *Org. Biomol. Chem.* **2010**, *8*, 1610.
16. Maiti, I. B.; Kolattukudy, P. E. *Science* **1979**, *205*, 507.
17. Shabab, M.; Shindo, T.; Gu, C.; Kaschani, F.; Pansuriya, T.; Chintha, R.; Harzen, A.; Colby, T.; Kamoun, S.; van der Hoorn, R. A. L. *Plant Cell* **2008**, *20*, 1169.
18. Koncz, C.; Schell, J. *Mol. Gen. Genet.* **1986**, *204*, 383.